ARTICLE

Photo-oxidation of Isoprene with Organic Seed: Estimates of Aerosol Size Distributions Evolution and Formation Rates

Yue Cheng, Chang-jin Hu, Yan-bo Gai, Xue-jun Gu, Wei-xiong Zhao, Wei Huang*, Wei-jun Zhang*

Lab of Atmospheric Physico-Chemistry, Anhui Institute of Optics and Fine Mechanics, Chinese Academy of Sciences, Hefei 230031, China

(Dated: Received on April 22, 2013; Accepted on June 8, 2013)

Indoor smog chamber experiments have been conducted to investigate the dynamics of secondary organic aerosol (SOA) formation from OH-initiated photo-oxidation of isoprene in the presence of organic seed aerosol. The dependence of the size distributions of SOA on both the level of pre-existing particles generated *in situ* from the photo-oxidation of trace hydrocarbons of indoor atmosphere and the concentration of precursor, has been investigated. It was shown that in the presence of high-level seed aerosol and low-level isoprene (typical urban atmospheric conditions), particle growth due to condensation of secondary organic products on pre-existing particles dominated; while in the presence of low-level seed aerosol and comparatively high-level isoprene (typical atmospheric conditions in rural region), bimodal structures appeared in the size distributions of SOA, which corresponded to new particle formation resulting from homogeneous nucleation and particle growth due to condensation of secondary organic products on the per-existing particles respectively. The effects of concentrations of organic seed particles on SOA were also investigated. The particle size distributions evolutions as well as the corresponding formation rates of new particles in different conditions were also estimated.

Key words: Photochemical reaction, Isoprene, Organic seed aerosol, Nucleation, Condensation

I. INTRODUCTION

Secondary organic aerosol (SOA), mainly formed from the atmospheric oxidation products of volatile organic compounds (VOCs), accounts for a significant fraction of ambient tropospheric aerosol. It is believed that SOA not only is of climatic interest as it can act as cloud condensation nuclei [1] or scatters and absorbs solar radiation [2], but also plays a key role in some environmental processes as it will lead to the formation of photochemical smog and the increase of ozone concentration in troposphere [3, 4]. Additionally, SOA may also have adverse effects on human health through its inhalation [5−7]. Understanding these effects requires a greater knowledge of the SOA formation mechanism in the atmosphere.

Numerous laboratory chamber studies and field investigations have shown that formation dynamics, yield and chemical composition of SOA are related to the environmental complexity [8]. Generally, it is believed that the presence of seed aerosol may offer condensation surfaces which affect the formation dynamics and yield of SOA. And the recent modeling studies of atmospheric aerosols using explicit chemical mechanisms based on results from simulation chamber experiments (traditionally with no background particles) have also shown a significant under-prediction of SOA formation when compared to measurements at the widespread presence of pre-existing particles in the real atmosphere [9]. Therefore, it is pivotal to learn the important role of seed aerosol in the formation of SOA. Historically, well-known inorganic aqueous solutions, for example, ammonium sulphate/sulphuric acid system, were used to produce homogeneous seed aerosol in most chamber experiments to study SOA formation [8]. Some recent studies have shown that the formation of SOA may also be significantly affected when organic seed aerosol is presented [10−12]. However, similar to the studies carried at the presence of inorganic seed particles, known homogeneous seed aerosols were used in these studies without considering the disparity between the chemical properties of the seed used in mimic smog chamber and that in real atmosphere. Thus, the studies with more suitable seed particles on the formation of SOA are imperative.

Bottom-up estimates show that the annual SOA production from biogenic volatile organic compounds (BVOCs) ranges from 2.5 Tg/yr to 44.5 Tg/yr, comprising about 60% of the organic aerosol mass on the global scale [13, 14]. Isoprene (2-methyl-1, 3-butadiene,

*Authors to whom correspondence should be addressed. E-mail: huangwei@aiofm.ac.cn, wjzhang@aiofm.ac.cn

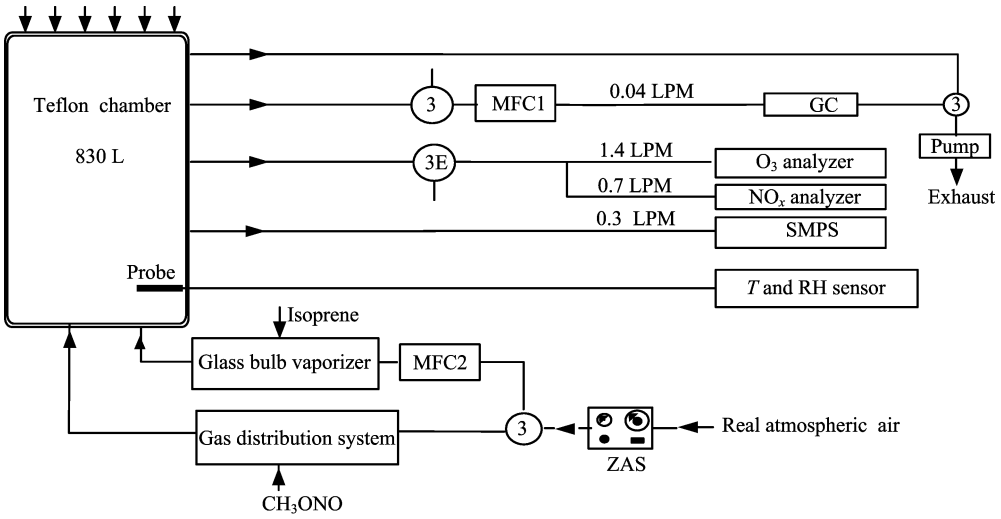

FIG. 1 Schematic of the experimental apparatus. 3: Three-way valve, E: electromagnetic valve.

C_5H_8), as the largest global biogenic emissions of non-methane VOCs, is estimated to be ∼600 Tg/yr [15]. Because of its two double bonds, isoprene is highly reactive and readily oxidized in the atmosphere by OH and other oxidants, which contributes substantially to the formation of SOA in the atmosphere [16, 17]. Surratt and coworkers investigated the effect of particle-phase acidity on SOA formation from isoprene, and found that increased acidity of inorganic seed aerosol leads to enhanced SOA formation [18, 19]. Dommen and coworkers determined the aerosol yield of isoprene oxidation in the presence of organic seed particles using carbon isotope analysis [11].

In the present work, the effect of organic seed aerosol, especially its surface concentration, on the formation dynamics of SOA resulting from OH-initialed photo-oxidation of isoprene was investigated in a home-made indoor smog chamber. Considering most organic aerosol in the real atmosphere is oxidized [20, 21], oxidized organic aerosol may be a better candidate as seed particle to simulate a real environment. So, *in situ* chamber generated SOA from photo-oxidation of real atmospheric volatile organic compounds was chosen as seed aerosol instead of conventional inorganic salts aerosol or a kind of known pure organic compound aerosol in this work.

II. EXPERIMENTS

To investigate the dependence of the size distributions of SOA on the level of organic seed particles and the concentration of precursor, a series of experiments were performed in a home-made collapsible chamber. Details of the chamber and its operation were described elsewhere [22, 23]. Briefly, it consists of three parts, including the sample introduction system, the main reactor, and the detection system, as shown in Fig.1. The main reactor is a ∼830 L (1.3 m×0.8 m×0.8 m) flexible bag made of 50 μm FEP Teflon film, where the photo-oxidations of trace hydrocarbons (HCs) or isoprene were carried out and aerosol particles were produced. Prior to each run, the chamber was evacuated by a mechanical pump and then flushed with purified air to full volume alternately at least 4 times to remove HCs, O_3, NO_x, moisture, and the particles. Purified air with no detectable non-methane hydrocarbons (NMHC<1 ppb), NO_x (<1 ppb), low O_3 concentration (<3 ppb), low particle densities (<5 particles/cm^3), and <10% relative humidity (RH), is supplied by a zero air supply (ZAS, TEI, model 111, USA) and generally used as carrier gas or background atmosphere in smog chamber. While in the experiments of investigating the effect of the organic seed aerosol produced *in situ* from the photo-oxidation of HCs in real atmospheric air, about 20% volume "semi-purified air" was introduced into the chamber. The component of the "semi-purified air" is almost the same as that of the purified air except the higher HCs. It is because that the heating reactor of the ZAS, where HCs are oxidized to CO_2 and water, was shut off when the "semi-purified air" was prepared so the trace HCs from ambient atmosphere were still kept. Methyl nitrite (CH_3ONO), as OH precursor, synthesized and purified prior to the experiments [23], was evaporated into the evacuated glass system and then flushed into the smog chamber using purified air in the dark condition in case of photo-dissociation. Isoprene (>99%, Alfa Aesar) was firstly injected into a 250 mL temperature-controlled glass bulb vaporizer (50−300 °C), and then flushed into the chamber by purified air.

Generally, each run of the experiments is typically split into three phases. In phase 1, the "semi-purified air" and methyl nitrite were well mixed in the main chamber, and then hydroxyl radicals were generated

DOI:10.1063/1674-0068/26/04/484-492

TABLE I Summary of the experimental conditions and the results.

Exp.	Isoprene/ppb	CH_3ONO/ppm	Organic seed			T/°C	RH/%	New particle	
			Surface/($\mu m^2/cm^3$)	Number/cm^{-3}	D_p[a]/nm			FR_{max}[b]	G_{NPF}[c]
R1	16.9	4.30	28.7	3.90×10^3	39.0	25.0	11.5	4.7×10^5	76
R2	12.4	4.50	<1.0	<5.0	N/A[d]	25.0	15.0	2.0×10^5	100
U1	31.0	4.30	613.0	3.25×10^4	69.5	26.0	14.0	N/A[d]	0
U2	624.7	4.30	613.0	3.28×10^4	69.5	26.1	13.7	1.8×10^6	45
S1	179.5	4.30	389.0	2.50×10^4	57.3	24.5	16.9	N/A[d]	0
S2	183.4	4.70	314.0	1.06×10^4	81.7	26.0	16.0	8.2×10^4	44
S3	179.6	4.80	122.0	4.89×10^3	75.6	26.0	14.8	1.3×10^6	81
S4	186.1	4.30	25.8	659.0	87.8	25.6	14.7	1.3×10^6	91

[a] D_p indicates particles mobility diameter.
[b] FR (in $cm^{-3}s^{-1}$) indicates the formation rate of new particles.
[c] G_{NPF} (in %) is defined as the ratio of volume concentration of new particles to total volume concentration.
[d] N/A: not applicable.

from the photolysis of methyl nitrite in air at wavelengths longer than 300 nm when the black lights were switched on [24], and the photo-oxidation of the trace HCs was initiated almost at the same time. As the reaction proceeded, aerosol formation from the photo-oxidation of trace HCs in the "semi-purified air" was investigated. In phase 2, when the size distribution of the aerosol in the chamber is stabilized (generally about 2 h later), the radiation lights were turned off. Then the concentration of the aerosol inside the chamber was diluted to a desired value (25.8−613.0 $\mu m^2/cm^3$) by purified air, which will act as the organic seed aerosol in the following experiment. No change in seed particle size was seen during dilution. In phase 3, after a certain concentration of isoprene has been injected into the chamber, the lights were turned on again to allow for the photo-oxidation of isoprene [25]. The effect of the organic seed aerosol on the formation dynamics of SOA from photo-oxidation of isoprene was studied by investigating the time evolution of isoprene and the formation of SOA as a function of time.

Isoprene, the precursor of SOA, was monitored by gas chromatography-flame ionization detector (GC-FID, Agilent 7820A, USA). The calibration of the concentration of isoprene was performed prior to each experiment by vaporizing some microliter volumes of a sample solution into an 80 L Teflon bag filled with a determined volume of purified air [26]. The aerosol size distributions from 14 nm to 673 nm were measured using a scanning mobility particle sizer (SMPS, TSI, 3936, USA), which consists of a TSI model 3077 ^{85}Kr neutralizer, a TSI model 3081 long column cylindrical differential mobility analyzer (DMA), and a TSI model 3775 condensation particle counter (CPC). The temperature and RH in the smog chamber are detected continually by a temperature and humidity sensor (Vaisala HMT333, Finland), and the concentrations of ozone and NO-NO_2-NO_x are measured by ozone analyzer (TEI, model 49i, USA) and NO-NO_2-NO_x analyzer (TEI, model 42i, USA) respectively.

As shown in Table I, three types of experiments were carried out to investigate SOA formation from the OH-initiated isoprene photo-oxidation under pre-existing organic seed aerosol conditions. In experiments R1 and R2, SOA formations under remote rural atmospheric conditions were measured. In experiments U1 and U2, the formations of SOA under simulated urban atmospheric particulate conditions were studied. While in experiments S1−S4, the effects of concentration of organic seed aerosol on the formations of SOA were investigated. In all the experiments, temperature and RH was 25.6±0.6 °C and 14.5±1.7% respectively, and 6 black lamps were used to irradiate the photochemical reactor.

III. RESULTS AND DISCUSSION

A. SOA formation from the OH-initiated photo-oxidation of isoprene under remote rural atmospheric conditions

The near ground-level concentrations of measured isoprene were from 0.3 ppbv to 10.2 ppbv in rural regions [27]. In the typical rural simulation experiment R1, following near complete reaction of the trace HCs from the "semi-purified air" with OH radicals, the chamber was diluted to leave the organic seed aerosol background of 28.7 $\mu m^2/cm^3$, and then 16.9 ppb isoprene was injected. The corresponding time-resolved number-weighted size distributions of SOA are illustrated in Fig.2(a), in which the left vertical red dotted line shows the end of phase 1 and the beginning of phase 2, while the right one shows the end of phase 2 and the beginning of phase 3, as discussed in experimental section. It was shown that firstly the size of SOA increased immediately following the injection of isoprene (indicated by the green arrowhead), and the

DOI:10.1063/1674-0068/26/04/484-492

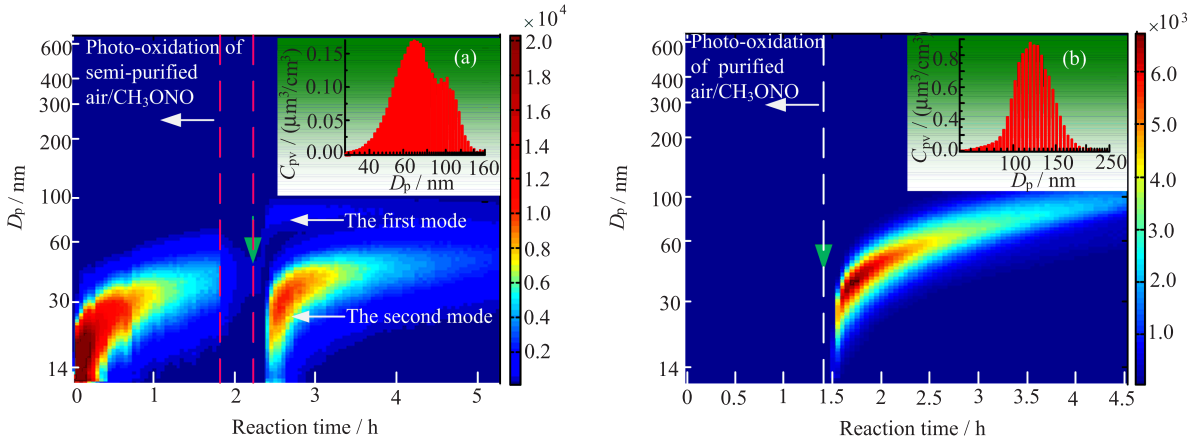

FIG. 2 Typical time-resolved number-weighted size distributions of experiment (a) R1 and (b) R2 under remote rural atmospheric conditions. The vertical red dotted lines show the division of the 3 different phases of the experiment and the green arrowheads indicate the injection of isoprene. C_{PV} is particle volume concentration.

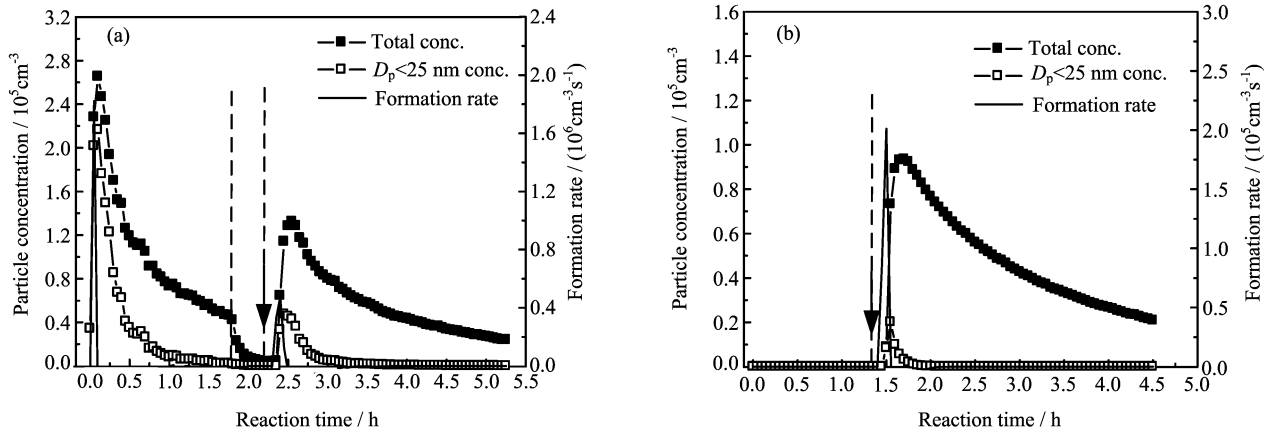

FIG. 3 The evolution of total number concentrations and number concentrations of the particles with diameters <25 nm as well as the formation rates of new particles of experiment (a) R1 and (b) R2.

distribution of which mainly presented in the size range of 60−100 nm, forming the Aitken mode. It is believed that this mode is related to the condensational growth of seed particles resulting from the partitioning of the oxidation products of isoprene onto the organic seed aerosol. While about 9 min later, another mode appeared. As this new mode starts in the nucleation mode, whose sizes are lower than our instrumentation's detection limit (14 nm), and keeps growth over a long time span, it is supposed this nucleation burst is a new particle formation (NPF) [28]. In order to validate this, the experiment R2 has been performed roughly by the same procedure and at the same condition, except that purified air are introduced into the chamber instead of "semi-purified air" in phase 1 of this run. As shown in Fig.2(b), it is obvious that there are no aerosol particles produced in phase 1, which means there are no seed organic aerosol particles in this run. And after the injection of isoprene, a clear nucleation burst is still observed, which validates the new particle formation of the second mode in R1.

In principle, a new particle mode appeared in the sub-25 nm size range are considered to be caused by formation of new particles from precursor vapor [29]. Thus, the particle formation rate in this work was derived from the rate of change of the number concentration of aerosols with diameters <25 nm. The evolution of total number concentrations and number concentrations of the particles with diameters <25 nm as well as the formation rate of new particles resulting from Fig.2 is shown accordingly to Fig.3. In Fig.3(a), the first new particle formation was observed following the oxidation of the trace HCs in "semi-purified air", and the second intensive NPF event appeared after the injection of isoprene with rate as high as 4.7×10^5 $cm^{-3}s^{-1}$, which shows consistence with that in Fig.3(b) (see also in Table I).

When seed particles are presented, the reaction products will either condense onto pre-existing particles or nucleate to form new particles. The ratio of volume

DOI:10.1063/1674-0068/26/04/484-492

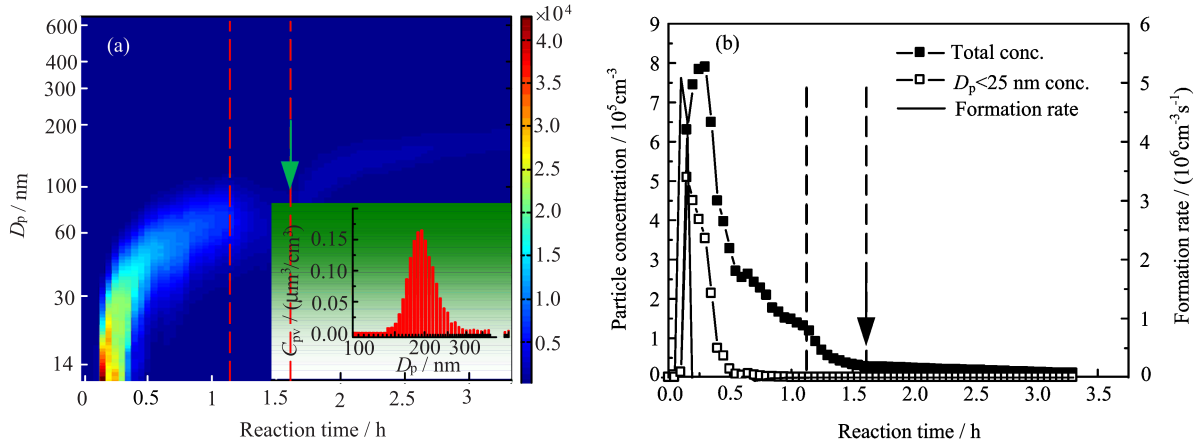

FIG. 4 (a) Typical time-resolved number-weighted size distributions and (b) the formation rate of new particles with diameters <25 nm of experiment U1 under simulated urban atmospheric particulate conditions.

concentration of new particles to total volume concentration, defined as G_{NPF}, is introduced to value the sink of the oxidation products of isoprene (see Table I). The steady size distributions at the end of the reaction of isoprene (the insets in Fig.2, and also see in the other time-resolved size distribution contour in the following text) were chosen to evaluate volume concentration of new particles and that of total particles. In experiment R2, almost all of the reaction products with low vapor pressure contribute to the formation and growth of the new particles, G_{NPF} is about 100%. Although the concentration of seed particles present in experiment R1 is 3.90×10^3 particles/cm^3, G_{NPF} is still as high as 76%. It was demonstrated that NPF dominated in simulated rural atmospheric conditions.

B. SOA formation from the OH-initiated photo-oxidation of isoprene under simulated urban atmospheric particulate conditions

Generally, the particulate concentration in urban atmosphere is the level of 10^4 particles/cm^3 with a number mean diameter of less than 100 nm. During the experiment period, the particulate concentration and size distribution of ambient atmosphere were measured using a scanning mobility particle sizer (SMPS) on July 31, 2012, in urban regions of Hefei, Anhui province of China. The temperature range of ambient atmosphere was from 29 °C to 37 °C. The measured particulate size range is from 14 nm to 673 nm and the sampling flow rate of SMPS is 0.3 L/min. It was shown that the number was in the range of $(0.5-3.5)\times10^4$ particles/cm^3 from 8:00 to 20:00, and the peak size was around 71.0 nm, which acted as the prototype of urban atmospheric particulate matter condition in this work. In the experiments U1 and U2, following near complete reaction of the trace HCs from the "semi-purified air" with OH radicals, the chamber was diluted until the concentration of the organic seed aerosol (peak particle size: 69.5 nm) was decreased to $(3.25-3.28)\times10^4$ particles/cm^3 with surface area of 613.0 μm^2/cm^3 corresponding to typical urban atmospheric particulate matter conditions, and then isoprene was injected.

In experiment U1, following the introduction of 31.0 ppb of isoprene, only the growth of seed particles are observed, and the size distribution always presents narrow single mode (Fig.4(a) and the insert). It is also shown in Fig.4(b) that there is no change of total number concentrations and no discernible nucleation event in phase 3 following the injection of isoprene. As the narrowing of the size distribution, the particle growth is a characteristic feature of condensational growth [30], it is believed that the less volatile oxidation products incline to the condensation on seed particles in this case. When high level isoprene with the initial concentration of 624.7 ppb was introduced, however, more complicated size distributions were presented (Fig.5). Besides the condensational growth of the seed organic particles similar to that appeared in U1, a significant nucleation burst was observed about 20 min later with the maximum formation rate up to 1.8×10^6 particles/(cm^{3}s). And the ratio of volume concentration of new particles to total volume concentration, G_{NPF}, is about 45% in this case. It is believed that the surface area provided by the pre-existing particles was insufficient to quench nucleation, which resulted in the new particle formation. It is worth pointing out that there is a third minor but detectable growth mode with the diameter in the range of 60−100 nm. It is interesting that Chen and coworkers also found the similar mode in ambient aerosol measurements from Atlanta, but the nature of this mode is still unclear and further study is needed in order to characterize this mode [31].

DOI:10.1063/1674-0068/26/04/484-492

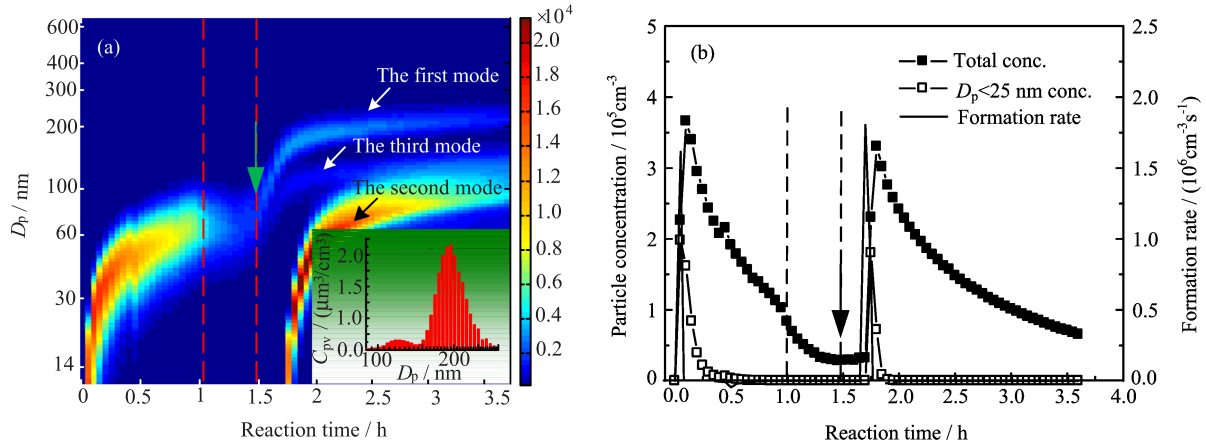

FIG. 5 (a) Typical time-resolved number-weighted size distributions and (b) the formation rate of new particles with diameters <25 nm of experiment U2 under simulated urban atmospheric particulate conditions.

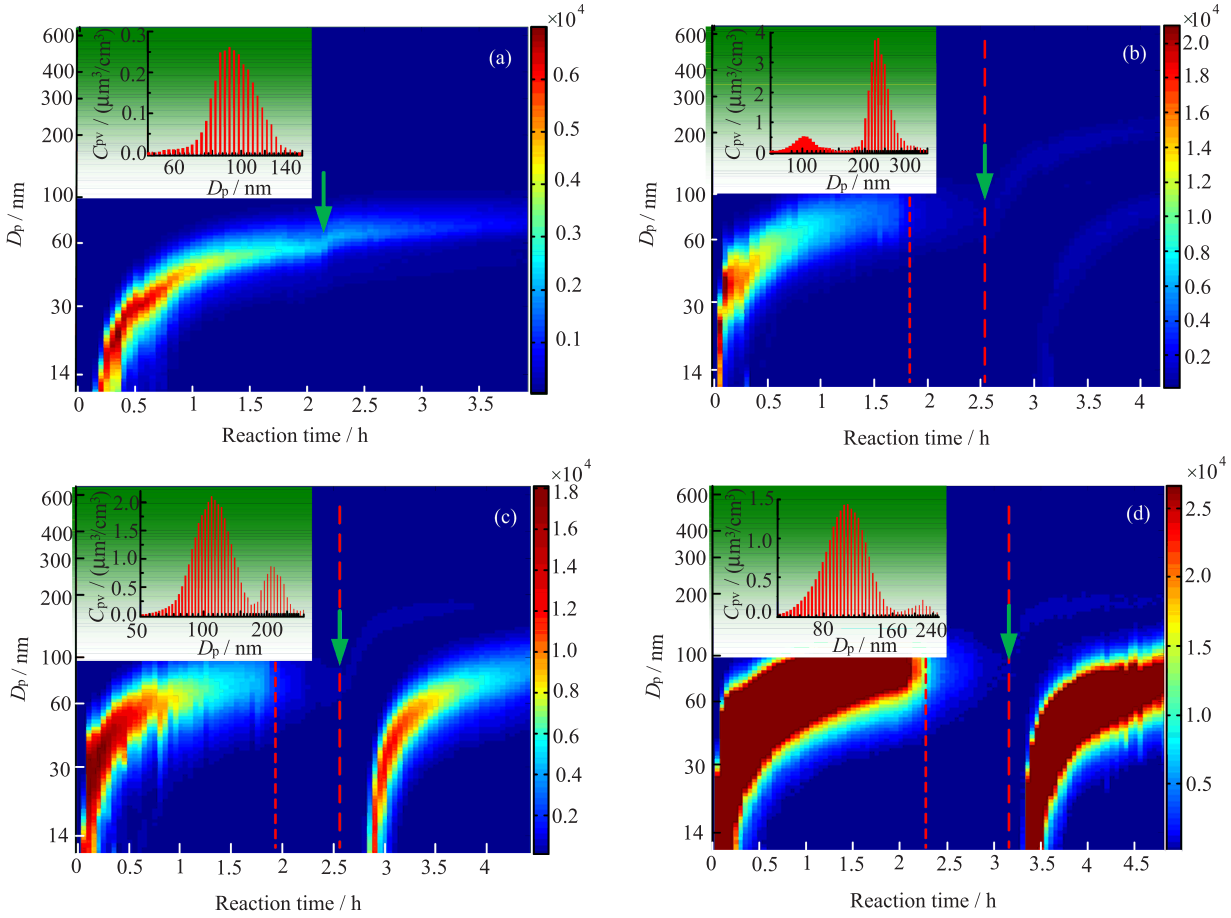

FIG. 6 Typical time-resolved number-weighted size distributions of experiment (a) S1, (b) S2, (c) S3, and (d) S4 under organic seed aerosol with different surface area concentrations conditions. The concentration of the injected isoprene was 182.2±3.2 ppb.

C. The effects of concentrations of organic seed particles on size distributions evolution and formation rates of SOA formation from the OH-initiated photo-oxidation of isoprene

In order to measure the effects of surface area concentrations of organic seed particles on the formation of SOA, a series of experiments (S1−S4) were carried out. In experiments S1−S4, the concentrations of the initial isoprene were kept almost the same (182.2±3.2 ppb), while the surface area concentrations of organic seed particles ranged from 25.8 $\mu m^2/cm^3$ to 389.0 $\mu m^2/cm^3$

DOI:10.1063/1674-0068/26/04/484-492

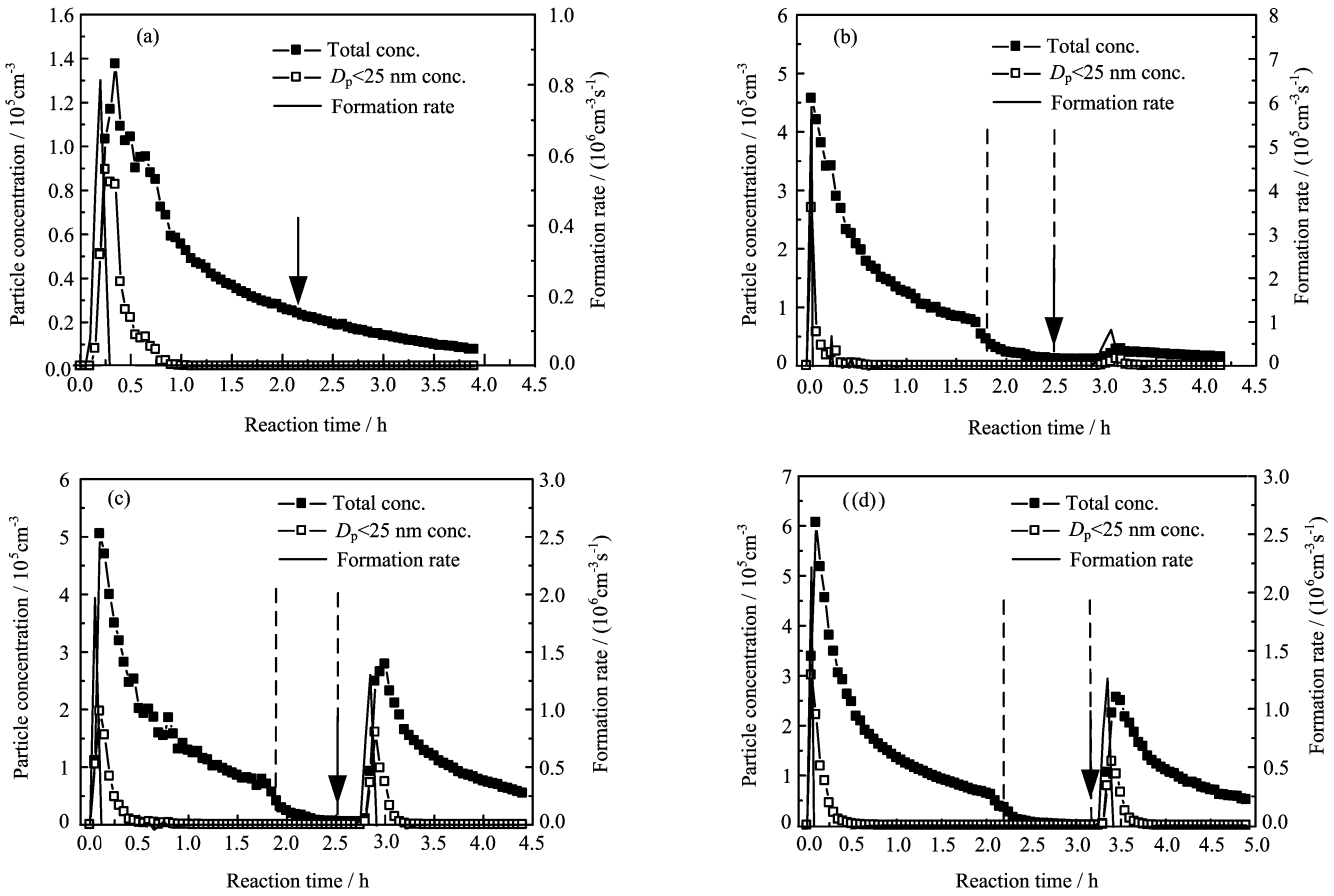

FIG. 7 The evolution of total number concentrations and number concentrations of the particles with diameters <25 nm as well as the formation rates of new particles of experiment (a) S1, (b) S2, (c) S3, and (d) S4.

(see Table I). The time-resolved number-weighted size distributions of SOA in S1−S4 are illustrated in Fig.6, and the corresponding evolution of total number concentrations, number concentrations of the particles with diameters <25 nm and the formation rates of new particles are presented in Fig.7. In experiment S1, when the surface area of the organic seed particle was high to 389.0 $\mu m^2/cm^3$, only condensational growth of seed particles was observed and no new particles were produced following the injection of isoprene, so the size distribution showed unimodal with peak at 91.4 nm (Fig.6(a) and Fig.7(a)). However, in experiments S2−S4, when the surface area provided by the pre-existing particles was insufficient to quench nucleation, new particles were formed and became more and more important according to the decreasing of the surface area concentrations of seed particles, which can be seen readily from the change of the relative intensity of the two mode as shown in Fig.6 (b)−(d). NPF along with the changing of the surface area concentrations of seed particles has also been demonstrated by the evolution of total number concentrations and the formation rates of new particles shown in Fig.7 (b)−(d). As shown in Table I, when the surface area concentrations of seed particles decrease from 389.0 $\mu m^2/cm^3$ to 25.8 $\mu m^2/cm^3$, new particle formation rates increase from 0 to 1.3×10^6 particles/(cm^3s) and G_{NPF} from 0 to 91%. Given the spherical shape of seed particles, the surface area concentration of seed particles is a function of number concentrations and diameter of particles. As it is difficult to control the size distribution at the same range in different runs, we can not differentiate the diameter-effect from the surface-area-effect. And it is also important to note that the initial concentration of isoprene precursor is higher than the real level in ambient atmosphere, which is in favor of the nucleation of new particles. However, qualitative trend of the surface area concentrations of seed particles on the formation of SOA is reliable taking account of the roughly same initial concentration of isoprene. Thinking about the complexity of the real atmosphere, for example, "complex pollution" in many Chinese cities, learning the effect of *in situ* produced organic seed particles on the formation of SOA is valuable and meaningful to learn the formation and growth of SOA in real atmosphere. Actually, some recent field measurements have demonstrated that aerosol in haze events exhibited complicated size distributions characteristics. Although the nature of these

DOI:10.1063/1674-0068/26/04/484-492

characteristics is still unclear, it is proposed that the size distributions of aerosol are related to the complexity of the atmosphere [32−34].

IV. CONCLUSION

Rather that use a conventional seed aerosol containing ammonium sulfate or homogeneous known organic aerosol, *in situ* generated SOAs from photo-oxidation of HCs in real atmospheric air have been used as seed particles to study its effect on the formation and growth of SOA from the OH-initiated photo-oxidation of isoprene in this work. Three different series of indoor smog chamber experiments were performed to study SOA formation and growth under typical urban atmospheric particulate conditions and remote rural atmospheric conditions, as well as the different concentrations of organic seed particles. The effect of surface area concentrations of organic seed aerosol on size distributions and new particle formation rates of SOA has been demonstrated. These studies may provide important insights into atmospheric aerosol dynamics, including formation mechanism of aerosol bimodal size distributions and formation rates of new particles in real atmosphere.

V. ACKNOWLEDGEMENTS

This work was supported by the State Key Program of National Natural Science Foundation of China (No.21133008), the National Natural Science Foundation of China (No.40975080, No.10979061, and No.41175121), the Natural Science Foundation of Anhui Province of China (No.1208085MD59), and the Foundation of Director of Anhui Institute of Optics and Fine Mechanics, Chinese Academy of Sciences (No.YO3AG31147).

[1] T. Novakov and J. E. Penner, Nature **365**, 823 (1993).
[2] M. O. Andreae and P. J. Crutzen, Science **276**, 1052 (1997).
[3] S. H. Chung and J. H. Seinfeld, J. Geophys. Res. **107**, 4407 (2002).
[4] J. H. Seinfeld, T. E. Kleindienst, E. O. Edney, and J. B. Cohen, Aerosol Sci. Technol. **37**, 728 (2003).
[5] D. W. Dockery, C. A. Pope, X. P. Xu, J. D. Spengler, J. H. Ware, M. E. Fay, B. G. Ferris, and F. E. Speizer, New England J. Med. **329**, 1753 (1993).
[6] C. A. Pope, M. J. Thun, M. M. Namboodiri, D. W. Dockery, J. S. Evans, F. E. Speizer, and C. W. Heath, Am. J. Respir. Crit. Care Med. **151**, 669 (1995).
[7] K. A. Miller, D. S. Siscovick, L. Sheppard, K. Shepherd, J. H. Sullivan, G. L. Anderson, and J. D. Kaufman, New England J. Med. **356**, 447 (2007).
[8] M. Hallquist, J. C. Wenger, U. Baltensperger, Y. Rudich, D. Simpson, M. Claeys, J. Dommen, N. M. Donahue, C. George, A. H. Goldstein, J. F. Hamilton, H. Herrmann, T. Hoffmann, Y. Iinuma, M. Jang, M. E. Jenkin, J. L. Jimenez, A. K. Scharr, W. Maenhaut, G. McFiggans, T. F. Mentel, A. Monod, A. S. H. Prevot, J. H. Seinfeld, J. D. Surratt, R. Szmigielski, and J. Wildt, Atmos. Chem. Phys. **9**, 5155 (2009), and references therein.
[9] R. Volkamer, J. L. Jimenez, F. San Martini, K. Dzepina, Q. Zhang, D. Salcedo, L. T. Molina, D. R. Worsnop, and M. J. Molina, Geophys. Res. Lett. **33**, L17811 (2006).
[10] R. Volkamer, P. J. Ziemann, and M. J. Molina, Atmos. Chem. Phys. **9**, 1907 (2009).
[11] J. Dommen, H. Helleun, M. Saurer, M. Jaeggi, R. Siegwolf, A. Metzger, J. Duplissy, M. Fierz, and U. Baltensperger, Environ. Sci. Technol. **43**, 6697 (2009).
[12] J. F. Hamilton, M. R. Alfarra, K. P. Wyche, M. W. Ward, A. C. Lewis, G. B. McFiggans, N. Good, P. S. Monks, T. Carr, I. R. White, and R. M. Purvis, Atmos. Chem. Phys. **11**, 5917 (2011).
[13] K. Tsigaridis and M. Kanakidou, Atmos. Chem. Phys. **3**, 1849 (2003).
[14] M. Kanakidou, J. H. Seinfeld, S. N. Pandis, I. Barnes, F. J. Denterner, M. C. Facchini, R. V. Dingenen, B. Ervens, A. Nenes, C. J. Nielsen, E. Swietlicki, J. P. Putaud, Y. Balkanski, S. Fuzzi, J. Horth, G. K. Moortgat, R. Winterhalter, C. E. L. Myhre, K. Tsigaridis, E. Vignati, E. G. Stephanou, and J. Wilson, Atmos. Chem. Phys. **5**, 1053 (2005).
[15] A. Guenther, T. Karl, P. Harley, C. Wiedinmyer, P. I. Palmer, and C. Geron, Atmos. Chem. Phys. **6**, 3181 (2006).
[16] M. Claeys, B. Graham, G. Vas, W. Wu, R. Vermeylen, V. Pashynska, J. Cafmeyer, P. Guyon, M. O. Andreae, P. Artaxo, and W. Maenhaut, Science **303**, 1173 (2004).
[17] A. G. Carlton, C. Wiedinmyer, and J. H. Kroll, Atmos. Chem. Phys. **9**, 4987 (2009).
[18] J. D. Surratt, M. Lewandowski, J. H. Offenberg, M. Jaoui, T. E. Kleindienst, E. O. Edney, and J. H. Seinfeld, Environ. Sci. Technol. **41**, 5363 (200).
[19] J. D. Surratt, A. W. H. Chan, N. C. Eddingsaas, M. N. Chan, C. L. Loza, A. J. Kwan, S. P. Hersey, R. C. Flagan, P. O. Wennberg, and J. H. Seinfeld, Proc. National Acad. Sci. **107**, 6640 (2010b).
[20] J. L. Jimenez, M. R. Canagaratna, N. M. Donahue, A. S. H. Prevot, Q. Zhang, J. H. Kroll, P. F. DeCarlo, J. D. Allan, H. Coe, N. L. Ng, A. C. Aiken, K. S. Docherty, I. M. Ulbrich, A. P. Grieshop, A. L. Robinson, J. Duplissy, J. D. Smith, K. R. Wilson, V. A. Lanz, C. Hueglin, Y. L. Sun, J. Tian, A. Laaksonen, T. Raatikainen, J. Rautiainen, P. Vaattovaara, M. Ehn, M. Kulmala, J. M. Tomlinson, D. R. Collins, M. J. Cubison, E. J. Dunlea, J. A. Huffman, T. B. Onasch, M. R. Alfarra, P. I. Williams, K. Bower, Y. Kondo, J. Schneider, F. Drewnick, S. Borrmann, S. Weimer, K. Demerjian, D. Salcedo, L. Cottrell, R. Griffin, A. Takami, T. Miyoshi, S. Hatakeyama, A. Shimono, J. Y. Sun, Y. M. Zhang, K. Dzepina, J. R. Kimmel, D. Sueper, J. T. Jayne, S. C. Herndon, A. M. Trimborn, L. R. Williams, E. C. Wood, A. M. Middlebrook, C. E. Kolb, U. Baltensperger, and D. R. Worsnop, Science **326**, 1525 (2009).
[21] Q. Zhang, J. L. Jimenez, M. R. Canagaratna, J. D. Allan, H. Coe, I. Ulbrich, M. R. Alfarra, A. Takami,

DOI:10.1063/1674-0068/26/04/484-492

A. M. Middlebrook, Y. L. Sun, K. Dzepina, E. Dunlea, K. Docherty, P. F. DeCarlo, D. Salcedo, T. Onasch, J. T. Jayne, T. Miyoshi, A. Shimono, S. Hatakeyama, N. Takegawa, Y. Kondo, J. Schneider, F. Drewnick, S. Borrmann, S. Weimer, K. Demerjian, P. Williams, K. Bower, R. Bahreini, L. Cottrell, R. J. Griffin, J. Rautiainen, J. Y. Sun, and Y. M. Zhang, Geophys. Res. lett. **34**, L13801 (2007).

[22] G. Pan, C. J. Hu, Z. Y. Wang, Y. Cheng, Y. H. Zheng, X. J. Gu, W. X. Zhao, W. J. Zhang, J. Chen, F. Y. Liu, X. B. Shan, and L. S. Sheng, Rapid Commun. Mass Spectrom. **26**, 189 (2012).

[23] M. Q. Huang, W. J. Zhang, L. Q. Hao, Z. Y. Wang, W. W. Zhao, X. J. Gu, X. Y. Guo, X. Y. Liu, B. Long, and L. Fang, J. Atmos. Chem. **58**, 237 (2007).

[24] L. Q. Hao, Z. Y. Wang, M. Q. Huang, S. X. Pei, Y. Yang, and W. J. Zhang, J. Environ. Sci. **17**, 912 (2005).

[25] B. Verheggen, M. Mozurkewich, P. Caffrey, G. Frick, W. Hoppel, and W. Sullivan, Environ. Sci. Technol. **41**, 6046 (2007).

[26] J. R. Odum, T. Hoffmann, F. Bowman, D. Collins, R. C. Flagan, and J. H. Seinfeld, Environ. Sci. Technol. **30**, 2580 (1996).

[27] C. Wiedinmyer, S. Friedfeld, W. Baugh, J. Greenberg, A. Guenther, M. Fraser, and A. Allen, Atmos. Environ. **35**, 1001 (2001).

[28] M. Dal Maso, M. Kulmala, I. Riipinen, R. Wagner, T. Hussein, P. P. Aalto, and E. J. Lehtinen, Boreal Environ. Res. **10**, 323 (2005).

[29] M. Kulmala, Tellus. **53B**, 324 (2001).

[30] J. H. Seinfeld, Atmos. *Chemistry and Physics of Air Pollution*, New York: Wiley-Interscience, (1986).

[31] M. Chen, M. Titcombe, J. K. Jiang, C. Jen, C. G. Kuang, M. L. Fischer, F. L. Eisele, J. I. Siepmann, D. R. Hanson, J. Zhao, and P. H. McMurry, Proc. National Acad. Sci. **109**, 18713 (2012).

[32] G. H. Wang, K. Kawamura, M. J. Xie, S. Y. Hu, J. J. Cao, Z. S. An, J. G. Waston, and J. C. Chow, Environ. Sci. Technol. **43**, 6493 (2009).

[33] A. Waheed, X. L. Li, M. G. Tan, L. M. Bao, J. F. Liu, Y. X. Zhang, G. L. Zhang, and Y. Li, Aerosol Sci. Technol. **45**, 163 (2011).

[34] R. Xiao, N. Takegawa, M. Zheng, Y. Kondo, Y. Miyazaki, T. Miyakawa, M. Hu, M. Shao, L. Zeng, Y. Gong, K. Lu, Z. Deng, Y. Zhao, and Y. H. Zhang, Atmos. Chem. Phys. **11**, 6911 (2011).

DOI:10.1063/1674-0068/26/04/484-492